

The R_{AA} and v_2 of muons from heavy-quark decays in Pb+Pb collisions at $\sqrt{s_{NN}} = 2.76$ TeV with the ATLAS detector

Alexander Milov for the ATLAS Collaboration

Weizmann Institute of Science, 234 Herzl Street, Rehovot 7610001 Israel

Abstract

The ATLAS experiment measures the production of muons coming from the decays of heavy flavour particles in the kinematic interval $4 < p_T < 14$ GeV and $|\eta| < 1$. The measurement is performed in $\sqrt{s} = 2.76$ TeV pp collisions and over the centrality range of (0–60)% in $\sqrt{s_{NN}} = 2.76$ TeV Pb+Pb collisions. The heavy flavour muon differential cross-sections and per-event yields are measured in pp and Pb+Pb collisions, respectively. The nuclear modification factor measured in 0–10% most central collisions is observed to be approximately equal to 0.4 and independent of p_T within uncertainties, which indicates suppressed production of heavy flavour muons in Pb+Pb collisions. The muon yields are also measured as a function of the azimuthal angle with respect to the event plane. Fourier coefficients associated with the second harmonic modulation vary slowly with p_T and show a systematic variation with centrality that is characteristic of other elliptic anisotropy measurements.

Keywords: Nuclear modification factor, Azimuthal anisotropy, Heavy flavour, Centrality

1. Introduction

Heavy quarks provide an important probe of the properties of the quark-gluon plasma created in high-energy nuclear-nuclear collisions [1, 2, 3, 4, 5, 6, 7]. Heavy quarks, with the mass exceeding the temperature of the surrounding plasma $T \sim 200$ –500 MeV [8] are mostly produced early in the collision. Their production rates that can be calculated using pQCD, and their subsequent interactions reflect themselves in experimentally observable signatures. At high transverse momenta, greater than the quark mass, heavy quarks are thought to lose energy similar to light quarks but with mass-dependent modifications to the pattern of collisional and radiative energy loss [9, 10, 11]. At lower transverse momenta the quarks are thought to diffuse in the plasma losing energy and partially thermalizing [12]. Interacting with the medium heavy quarks may acquire an azimuthal anisotropy due to the collective expansion of the medium. Past measurements of heavy flavour quarks at RHIC and the LHC using semi-leptonic decays [13, 14, 15, 16] and direct reconstruction of heavy flavour mesons [17, 18, 19] have shown both substantial suppression in the yield of heavy quarks due to energy loss and significant azimuthal anisotropy.

☆

Email address: alexander.milov@weizmann.ac.il ()

This proceeding presents ATLAS measurements of heavy flavour muon production measured over $|\eta| < 1$ ¹ using 0.14 nb⁻¹ of Pb+Pb data at $\sqrt{s_{NN}} = 2.76$ TeV and 4.0 pb⁻¹ of pp data at $\sqrt{s} = 2.76$ TeV, collected during LHC operation in 2011 and 2013, respectively. The measurements are performed for several intervals of collision centrality, characterized using the total transverse energy measured in the forward calorimeters, and for different p_T intervals spanning the range $4 < p_T < 14$ GeV.

The heavy flavour muon differential per-event yields in Pb+Pb collisions and differential cross-sections in pp collisions are used to calculate the heavy flavour muon R_{AA} as a function of p_T in different Pb+Pb centrality intervals. In addition, the heavy flavour muon v_2 is measured as a function of p_T and collision centrality using the event-plane method with the second-order event plane angle, Ψ_2 , measured in the forward calorimeters.

Heavy flavour muons are statistically separated from background muons resulting from pion and kaon decays and hadronic interactions using a variable that compares the momenta of the muons measured in the inner detector and muon spectrometer. Over the p_T range of the measurement, the residual irreducible contamination of non-heavy flavour muons to the measurement, is $\lesssim 1\%$ including contributions from J/ψ decays [20].

2. Data analysis

The measurements presented in this proceeding are obtained using the ATLAS muon spectrometer (MS), inner detector (ID), calorimeter, trigger and data acquisition systems. A detailed description of these detectors and their performance in pp collisions can be found in Ref. [21]. The Pb+Pb events selected for this analysis are required to have a reconstructed vertex and a time difference between the signals in two Minimum Bias Trigger Scintillator detectors of less than 5 ns. At least one reconstructed collision vertex is required in pp collisions. The centrality of Pb+Pb collisions is characterised by transverse energy measured in the ATLAS forward calorimeter (FCal). Results presented in this proceeding, are worked out for several intervals ordered from the most central to the most peripheral collisions: 0–10%, 10–20%, 20–30%, 30–40%, and 40–60%.

Muons used in this analysis are obtained by combining tracks reconstructed in the MS with the tracks measured in the ID. The tracks are required to have momentum $p > 3$ (1.2) GeV in the ID and the MS respectively and to satisfy criteria on the number of hits in ID that are the same for the pp and Pb+Pb data. Transverse and longitudinal impact parameters of the track with respect to a reconstructed event vertex are required to be less than 5 mm. Muons selected for this analysis are constrained at low p_T to be above 4 GeV by the dependence of the muon trigger and reconstruction efficiencies while at high p_T by the available statistics of the Pb+Pb data. The muon η interval is chosen for optimal muon performance. A total of 9.2 million (1.8 million) muons are reconstructed within these kinematic ranges from 8.7 million (1.8 million) events recorded using the Pb+Pb (pp) muon triggers.

The performance of the ATLAS detector and offline analysis in measuring muons is evaluated using Monte Carlo samples obtained from GEANT4-simulated [22] $\sqrt{s} = 2.76$ TeV pp dijet events produced with the PYTHIA event generator [23] (version 6.423 with parameters chosen according to the AUET2B tune [24]). To account for the large occupancy in the detector readout channels in central Pb+Pb collisions PYTHIA events were overlayed onto Pb+Pb collision events selected with the minimum-bias trigger. For both the pp and Pb+Pb measurements, the muon reconstruction efficiency increases by about 15% between $p_T = 4$ and 6 GeV above which it is approximately constant at ~ 0.87 and ~ 0.84 for the pp and Pb+Pb data, respectively. The Pb+Pb reconstruction efficiency is independent of centrality within uncertainties. The Pb+Pb muon trigger efficiency increases from 0.60 at $p_T = 4$ GeV to ~ 0.75 at 6 GeV, above which it is approximately constant. The pp muon trigger efficiency increases from 0.52 for $4 < p_T < 4.5$ GeV to 0.82 for $p_T > 5.5$ GeV, above which it remains constant.

¹ ATLAS uses a right-handed coordinate system with its origin at the nominal interaction point (IP) in the center of the detector and the z -axis along the beam pipe. The x -axis points from the IP to the center of the LHC ring, and the y -axis points upward. Cylindrical coordinates (r, ϕ) are used in the transverse plane, ϕ being the azimuthal angle around the beam pipe. The pseudorapidity is defined in terms of the polar angle θ as $\eta = -\ln \tan(\theta/2)$.

The muons measured in the pp and Pb+Pb data sets contain background from in-flight decays of pions and kaons, muons produced from the decays of particles produced in hadronic showers, and mis-associations of ID and MS tracks. Previous studies have shown that the signal and background contributions to the reconstructed muon sample can be discriminated statistically [20]. This analysis relies on the fractional momentum imbalance, $\Delta p/p_{\text{ID}}$, shown in Fig. 1 which quantifies the difference between the ID and MS measurements of the muon momentum after accounting for the energy loss of the muon in the calorimeters.

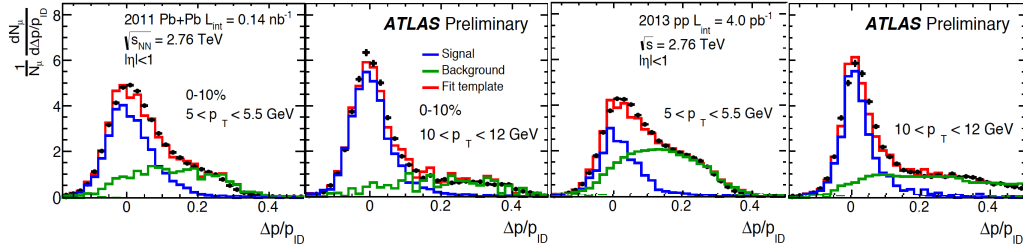


Fig. 1. Results of template fits to the 0–10% most central Pb+Pb collision data (left two panels) and to the pp collision data (right two panels) for two p_T ranges indicated in the panels. The black points represent the data, blue and green lines represent the signal and background template distributions and the red lines represent the combined template distributions. Figure from [25].

3. Results

The heavy flavour muon differential cross-section in pp and differential yields in Pb+Pb collisions are determined from the template fit procedure shown in Fig. 1. The measurement of the heavy flavour muon

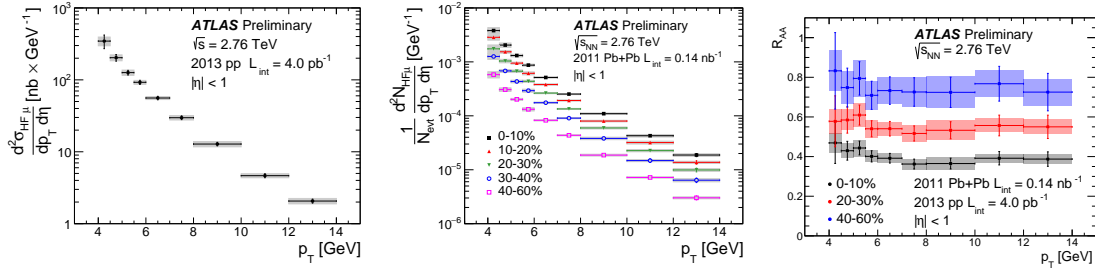


Fig. 2. Left: pp heavy flavour muon differential cross-section. Middle: Pb+Pb heavy flavour muon differential per-event yields. Right: heavy flavour muon R_{AA} measured as a function of p_T . The error bars represent statistical uncertainties on the data, while the systematic uncertainties, including the contribution from luminosity, are indicated by the shaded bands. Figure from [25].

differential cross-sections and per-event yields are subject to systematic uncertainties arising from the muon trigger selection, muon reconstruction efficiencies, the template fitting procedure, muon p_T resolution, and the pp luminosity explained in Ref. [25]. The results for pp and Pb+Pb are shown in Fig. 2 in the left and middle panels respectively. The right panel of the figure shows heavy-flavour muon R_{AA} , which decreases between peripheral (40–60%) and more central collisions reaching a value of ~ 0.4 in the 0–10% centrality interval. The measured R_{AA} appear to be p_T -independent within the uncertainties of the measurement. These results are consistent with previous results from the ALICE experiment [15], but have much smaller uncertainties.

The heavy flavour muon v_2 values are measured by evaluating the yields differentially with respect to the event plane. The extracted v_2 values, are then corrected to account for the event plane resolution. The sources of the systematic uncertainties in the v_2 measurements are mostly the same as those in the R_{AA} measurements, however, the trigger and tracking efficiencies do not have a significant effect on the v_2 . The

resolution-corrected v_2 values are plotted in the left panel of Fig. 3 as a function of p_T for several centrality intervals used in this analysis.

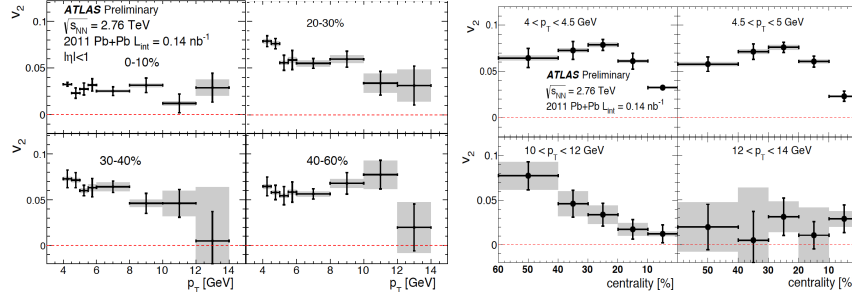


Fig. 3. The p_T dependence (left) and centrality dependence (right) of the heavy flavour muon v_2 . The error bars and shaded bands represent statistical and systematic uncertainties respectively. Figure from [25]

Over the 20–40% centrality range, the v_2 is largest at the lowest measured p_T of 4 GeV and decreases for higher p_T . However, in the 0–10% and 40–60% centrality intervals, no clear p_T dependence is visible. For all centralities, significant non-zero v_2 is observed even at p_T of 10 GeV. Right panels of the figure show the same set of results plotted as a function of centrality for different p_T intervals. For low p_T range the centrality dependence of the heavy flavour muon v_2 is qualitatively similar in shape, but considerably smaller in magnitude, to that for charged hadrons of similar p_T [26, 27]. In this p_T range, the v_2 first increases from central to mid-central events, reaches a maximum between 20–40% centrality, and then decreases. Over the p_T range of 8–12 GeV the v_2 increases monotonically from central to peripheral events. However, the associated statistical and systematic uncertainties are considerably larger. This monotonically increasing centrality dependence of the v_2 at high p_T is also seen in the inclusive charged hadron v_2 [26, 27]. For the highest p_T interval of $12 < p_T < 14$ GeV, the statistical and systematic errors are too large to clearly understand the centrality dependence of the v_2 .

References

- [1] H. van Hees, R. Rapp, Phys. Rev. C71 (2005) 034907. [arXiv:nucl-th/0412015](#).
- [2] C. P. Herzog, A. Karch, P. Kovtun, C. Kozcaz, L. G. Yaffe, JHEP 07 (2006) 013. [arXiv:hep-th/0605158](#).
- [3] H. van Hees, M. Mannarelli, V. Greco, R. Rapp, Phys. Rev. Lett. 100 (2008) 192301. [arXiv:0709.2884](#).
- [4] W. A. Horowitz, M. Gyulassy, Phys. Lett. B666 (2008) 320–323. [arXiv:0706.2336](#).
- [5] J. Uphoff, O. Fochler, Z. Xu, C. Greiner, Phys. Rev. C84 (2011) 024908. [arXiv:1104.2295](#).
- [6] M. He, R. J. Fries, R. Rapp, Phys. Rev. C86 (2012) 014903. [arXiv:1106.6006](#).
- [7] S. Cao, G.-Y. Qin, S. A. Bass, Phys. Rev. C88 (4) (2013) 044907. [arXiv:1308.0617](#).
- [8] N. Armesto, et al., J. Phys. G35 (2008) 054001. [arXiv:0711.0974](#).
- [9] M. Djordjevic, M. Gyulassy, Nucl. Phys. A733 (2004) 265–298. [arXiv:nucl-th/0310076](#).
- [10] P. B. Gossiaux, J. Aichelin, T. Gousset, V. Guiho, J. Phys. G37 (2010) 094019. [arXiv:1001.4166](#).
- [11] P. B. Gossiaux, J. Aichelin, J. Phys. G36 (2009) 064028. [arXiv:0901.2462](#).
- [12] G. D. Moore, D. Teaney, Phys. Rev. C71 (2005) 064904. [arXiv:hep-ph/0412346](#).
- [13] PHENIX Collaboration, A. Adare et al., Phys. Rev. Lett. 98 (2007) 172301. [arXiv:nucl-ex/0611018](#).
- [14] PHENIX Collaboration, A. Adare et al., Phys. Rev. C84 (2011) 044905. [arXiv:1005.1627](#).
- [15] ALICE Collaboration, B. Abelev et al., Phys. Rev. Lett. 109 (2012) 112301. [arXiv:1205.6443](#).
- [16] ALICE Collaboration, J. Adam et al. [arXiv:1507.03134](#).
- [17] ALICE Collaboration, B. Abelev et al., JHEP 09 (2012) 112. [arXiv:1203.2160](#).
- [18] ALICE Collaboration, B. Abelev et al., Phys. Rev. Lett. 111 (2013) 102301. [arXiv:1305.2707](#).
- [19] ALICE Collaboration, B. Abelev et al., Phys. Rev. C90 (3) (2014) 034904. [arXiv:1405.2001](#).
- [20] ATLAS Collaboration, Phys. Lett. B707 (2012) 438–458. [arXiv:1109.0525](#).
- [21] ATLAS Collaboration, JINST 3 (2008) S08003.
- [22] S. Agostinelli, et al., Nucl. Instrum. Meth. A506 (2003) 250–303.
- [23] T. Sjostrand, S. Mrenna, P. Z. Skands, JHEP 0605 (2006) 026. [arXiv:hep-ph/0603175](#).
- [24] ATLAS Collaboration, ATL-PHYS-PUB-2011-009, <http://cdsweb.cern.ch/record/1363300>.
- [25] ATLAS Collaboration, ATLAS-CONF-2015-053, <https://cds.cern.ch/record/2055674>.
- [26] ATLAS Collaboration, Phys. Lett. B707 (2012) 330–348. [arXiv:1108.6018](#).
- [27] ATLAS Collaboration, Phys. Rev. C86 (2012) 014907. [arXiv:1203.3087](#).